Applied Catalysis B: Environmental 166–167 (2015) 277–286

Contents lists available at ScienceDirect

Applied Catalysis B: Environmental

journal homepage: www.elsevier.com/locate/apcatb

Chemical deactivation of H-BEA and Fe-BEA as NH_3-SCR catalysts—effect of potassium

Soran Shwan [a,*], Jonas Jansson [b], Louise Olsson [a], Magnus Skoglundh [a]

[a] Competence Centre for Catalysis, Chalmers University of Technology, SE-412 96 Gothenburg, Sweden
[b] Volvo Group Trucks Technology, SE-40508 Gothenburg, Sweden

ARTICLE INFO

Article history:
Received 26 September 2014
Received in revised form
17 November 2014
Accepted 19 November 2014
Available online 26 November 2014

Keywords:
Potassium
Chemical deactivation
NH_3-SCR
Fe-BEA
XPS
NO_X adsorption.

ABSTRACT

H-BEA and Fe-BEA were experimentally studied for selective catalytic reduction of NO_X using ammonia (NH_3-SCR) with a focus on the chemical deactivation caused by potassium exposure where cordierite-supported H-BEA and Fe-BEA samples were exposed to 10 or 50 ppm KNO_3 for 14, 24 and 48 h in a continuous gas flow reactor at 350 °C. The samples were catalytically evaluated and characterized using a flow-reactor system and X-ray photoelectron spectroscopy.

The results show that new NO_X storage sites are formed on the expense of Brønsted acid sites for ammonia storage for all potassium-exposed samples. The formation of new NO_X storage sites results in increased NH_3-SCR activity for the potassium-exposed H-BEA samples. However, for the potassium-exposed Fe-BEA samples, the results show a significant decrease in SCR activity.

Deconvolution of the Fe $2p_{3/2}$ XPS peak shows a clear increase in the relative amount of Fe^{3+} for the potassium-exposed Fe-BEA samples, indicating that isolated iron species active for NH_3-SCR are exchanged with potassium, forming smaller trivalent iron clusters inside the zeolite pores. Transient experiments during NH_3-SCR show that the decrease in ammonia storage capacity due to potassium exposure results in a decreased period with improved NO reduction after NH_3 cut-off.

1. Introduction

Copper- [1–6] and iron- [2,7–11] exchanged zeolites can be used to eliminate nitrogen oxides (NO_X) under lean conditions for mobile applications. The technology for lean NO_X reduction is based on selective catalytic reduction using ammonia as reducing agent (NH_3-SCR) according to the stoichiometry in reaction (1) [7]:

$$NH_3 + 4NO + O_2 \rightarrow 4N_2 + 6H_2O \quad (1)$$

Copper-based zeolites are, in general, more active for low-temperature (<300 °C) SCR, while iron-based zeolites are more active at higher temperatures (>300 °C) during steady-state conditions. However, in real-world performance, steady-state conditions are rarely reached. Kamasamudram et al. [12] have shown that during transient conditions, when the ammonia supply varies, iron-exchanged zeolites achieve higher NO_X conversion than copper-exchanged zeolites.

With more stringent environmental legislations in many part of the world, the use of NH_3-SCR catalysts will increase as well as the usage of renewable fuels, especially biodiesel and other fuels from biomass. When using metal-exchanged zeolites in after treatment systems for diesel and lean burn vehicles, several challenges arise. Chemisorption of impurities (poisoning) on the active sites of the catalyst is one of the challenges [13]. Chemical poisoning of the catalyst results in decreased activity or selectivity, e.g. decreased NO_X reduction for the NH_3-SCR catalyst, hence metal-exchanged zeolites with resistance to impurities in biodiesel and lubricating oils such as calcium (Ca), magnesium (Mg), phosphorus (P), potassium (K), sulphur (S) and zinc (Zn) is desired [14,15]. Other challenges with metal-exchanged zeolites are hydrothermal stability [7] and hydrocarbon poisoning [16–18]. However, resistance to hydrocarbon poisoning has been shown to be enhanced significantly by addition of a protecting layer on the zeolite [16].

There are very few studies in the open literature of chemical deactivation focusing on metal-exchanged zeolites used for NH_3-SCR applications [15,19,20], whereas vanadia-based NH_3-SCR catalysts have been thoroughly investigated [15,20–26]. Most chemical deactivation studies in the open literature are performed using chemical impregnation (or doping) of the catalyst. However, it was concluded by Castellino et al. [23] that degradation of

* Corresponding author at: Competence Centre for Catalysis, Department of Applied Surface Chemistry, Chalmers University of Technology, SE-41296 Göteborg, Sweden. Tel.: +46 31 772 2943.
E-mail address: soran@chalmers.se (S. Shwan).

http://dx.doi.org/10.1016/j.apcatb.2014.11.042
0926-3373/

Table 1
Washcoat weight, relative amount of Fe^{3+} determined by XPS, NH_3 oxidation activity and increased NO_X reduction time after ammonia cut-off during NH_3-SCR for all samples.

Sample (KNO_3 exposure time and conc.)	Washcoat weight[a] (mg)	$Fe^{3+}/(Fe^{2+}+Fe^{3+})$ (%)	NH_3 oxidation at 500 °C (%)	Increased SCR period at 250 °C (min)	Increased SCR period at 300 °C (min)
Fe-BEA (fresh)	819	38	43	2.8	0.9
H-BEA (fresh)	**799**	**-**	**6**	**16**	**5.9**
14 h-10 ppm (Fe-BEA)	790	42	56	2.8	0.7
24 h-10 ppm (Fe-BEA)	792	44	41	2.5	0.6
48 h-10 ppm (Fe-BEA)	791	44	37	2.5	0.5
48 h-10 ppm (H-BEA)	**797**	**–**	**5**	**13**	**4.5**
14 h-50 ppm (Fe-BEA)	795	43	53	2.6	0.6
24 h-50 ppm (Fe-BEA)	804	46	38	3.0	0.7
48 h-50 ppm (Fe-BEA)	791	55	14	2.6	0.7
48 h-10 ppm (H-BEA)	**786**	**-**	**4**	**14**	**5.1**

[a] The mass of the cordierite substrate is not included in the washcoat weight.

vanadia-based SCR catalysts is much more severe when exposed to chemical impurities in the flue gas compared to wet-impregnation of the catalyst with impurities. Different studies of NH_3-SCR catalysts impregnated with phosphorous have correlated the decreased SCR activity with decreased NH_3 storage capacity. Silver et al. [20] concluded that exposure of iron-exchanged zeolites to phosphorous results in decreased SCR activity due to zeolite pore blockage and decreased NH_3 storage capacity. However, in a recent study by our group, the fundamental deactivation mechanisms of iron-exchanged zeolites due to exposure of iron-exchanged zeolite beta (Fe-BEA) to relatively low amounts of phosphorous under controlled flow-reactor experiments were studied [19]. It was found that metaphosphates (PO_3^-) are formed on the catalyst surface and exchanged with the hydroxyl groups on the active iron species resulting in decreased SCR activity. Furthermore, no correlation was found between the decreased NO_X reduction and the NH_3 storage capacity after phosphorous exposure.

The objective of the present study is to investigate the chemical deactivation of H-BEA and Fe-BEA as NH_3-SCR catalysts due to potassium exposure under controlled flow-reactor experiments. Kern et al. [15] showed strong decrease in NO_X reduction and NH_3 storage capacity of Fe-zeolites when wet-impregnated with potassium nitrate solution. However, the focus of the present work is on the fundamental deactivation mechanisms of the active iron species and hence relatively low amounts of potassium are used in the exposing gas of the catalysts. The fundamental deactivation mechanisms with focus on the active sites due to hydrothermal treatment and phosphorous exposure have recently been studied by our group [19,27–33]. The present study will continue the discussion related to the deactivation of the active sites with focus on potassium exposure.

2. Experimental methods

2.1. Sample preparation

H-BEA and 1 wt.% Fe-BEA were studied as NH_3-SCR catalysts in this study. The 1 wt.% Fe-BEA samples were prepared by incipient wetness impregnation, where 9.9 g of H-BEA powder (SAR = 38, Zeolyst International) was dried and mixed with 0.72 g of $Fe(NO_3)_3{\cdot}9H_2O$ (Fisher Scientific) dissolved in 9.9 ml of distilled water. The mixed solution was thereafter dried at 120 °C for 24 h and crushed into a fine powder before calcined in air at 450 °C for 3 h. Ten cordierite monolith substrates (Corning; 400 cpsi; 21 mm in diameter and 20 mm in length) were prepared and calcined in air at 500 °C for 2 h and washcoated with a layer of alumina (Disperal D, Sasol). The washcoated samples were then calcined at 500 °C for 2 h before the final catalyst washcoating. Seven samples were washcoated with 1 wt.% Fe-BEA and the other three were washcoated with H-BEA. Further details about the catalyst preparation can be found in refs. [19,31]. Table 1 shows the final amount of washcoat for the prepared samples.

2.2. Potassium exposure

The prepared H-BEA and Fe-BEA samples were exposed to potassium nitrate (KNO_3) using an ageing reactor which consists of a preheater and a reactor chamber placed vertically where up to six samples can be placed. Furthermore, thermocouples are placed in the front and the end of the pre-heater, and above each sample inside the reactor. Further details about the ageing reactor can be found in ref. [30].

During potassium exposure, the gas flow through the reactor was 4000 ml/min and consisted of 10 or 50 ppm KNO_3, and 10% H_2O, 6% O_2 and N_2 as inert gas with a space velocity (GHSV) of 5250 h^{-1}. Potassium nitrate was mixed with distilled water in the feed system of the ageing reactor. Thereafter, the diluted potassium nitrate solution was introduced to the pre-heater separately via a controlled evaporator mixer system (CEM, Bronkhorst Hi-Tech) and mixed with inert gas, heated to 350 °C and fed to the ageing reactor. Three Fe-BEA samples were exposed to 10 ppm KNO_3 at 350 °C for 14, 24 and 48 h, respectively. The other three Fe-BEA samples were exposed to 50 ppm of KNO_3 at 350 °C for 14, 24 and 48 h, respectively. Furthermore, two H-BEA samples were exposed to 10 and 50 ppm of KNO_3 for 48 h, respectively. One Fe-BEA and one H-BEA sample (denoted fresh) were kept untreated for comparison with the potassium-exposed samples.

Before any analysis, all samples (both fresh and potassium-exposed samples) were degreened in 400 ppm NO, 400 ppm NH_3, 8% O_2 and 5% H_2O at 500 °C for 2 h in another continuous flow-reactor system described in the following section.

The samples exposed to 10 ppm KNO_3 are referred to as 14 h 10 ppm, 24 h 10 ppm and 48 h 10 ppm, and the samples exposed to 50 ppm KNO_3 are referred to as 14 h 50 ppm, 24 h 50 ppm and 48 h 50 ppm in the figures.

2.3. Flow reactor system

A continuous flow-reactor system was used to characterize and evaluate the catalytic properties of all samples. The reactor system is further described in ref. [30]. Temperature-programmed desorption of ammonia, nitric oxide and nitrogen dioxide (NH_3-, NO- and NO_2-TPD, respectively), NO- and NH_3-oxidation, selective catalytic reduction of NO_X with ammonia (NH_3-SCR), and NH_3 inhibition experiments were performed using the reactor system. A gas mixing system consisting of separate mass flow controllers

(Bronkhorst) for NO, NH_3, O_2 and Ar was used. Water was added separately downstream of the mixed gases in an evaporator which was pre-heated to 150 °C. Furthermore, before each experiment in the flow-reactor, the samples were exposed to 8% O_2 in Ar at 500 °C for 15 min, and thereafter cooled to 150 °C.

During the NH_3-TPD experiments, the samples were exposed to 400 ppm of NH_3 and 5% H_2O at 150 °C for 40 min followed by flushing in 5% H_2O in Ar at the same temperature for another 30 min. After the flush, a temperature ramp in 5% water in Ar from 150 to 500 °C at a heating rate of 10 °C/min was performed. In addition to these experiments, NH_3-TPD experiments in the absence of water were performed for the fresh and potassium-exposed H-BEA samples.

Furthermore, NO-TPD follows the same procedure as the NH_3-TPD experiments but in the absence of water for all samples and using NO as probe molecule instead of ammonia.

Steady-state activity measurements (NH_3- and NO-oxidation and NH_3-SCR) were performed for all samples using 400 ppm NO and/or NH_3, 8% O_2 and 5% H_2O in Ar. The temperature was stepwise increased from 150 to 500 °C (150, 200, 250, 300, 400 and 500 °C) with a duration of 40 min for the first step, 30 min for step two and three, and 20 min for the last three steps. The heating rate between the temperature steps was 20 °C/min. Furthermore, during the ammonia inhibition experiments, the samples were exposed to NH_3-SCR conditions at 250 and 300 °C for 40 min before the ammonia feed was cut off. The SCR activity was continuously measured before and after the ammonia cut-off and inert gas was used to compensate and maintain constant flow. The total gas flow during all flow-reactor experiments was kept constant at 3500 ml/min which corresponds to a space velocity (GHSV) of 27,600 h^{-1}.

2.4. X-ray photoelectron spectroscopy

All H-BEA and Fe-BEA samples where characterized using X-ray photoelectron spectroscopy to determine the chemical state of potassium and iron in the samples. A Perkin Elmer PHI 5000C ESCA system described further in refs. [19,30] was used in this study. The experiments were performed by cutting out one of the inner channels of the washcoated monolith sample and placed in the XPS system. The K 2p, Fe 2p and O 1s binding energy levels were thoroughly studied and by normalizing the spectra using the C 1s peak at 285 eV [34] as reference correction for charging was performed. Furthermore, deconvolution of the Fe $2p_{3/2}$ peaks from each sample was performed by fitting a Gaussian function to the experimental data. The deconvoluted peak positions were optimized according to the same procedure for all samples to achieve the lowest standard deviation, χ^2, and found to be 709.5 and 712.2 eV for Fe^{2+} and Fe^{3+}, respectively. The fitted peaks are in accordance with other studies and summarized in Table 2.

3. Results

3.1. Temperature-programmed desorption of NH_3

The results from the temperature-programmed desorption experiments using NH_3 are shown in Figs. 1 and 2. Fig. 1 shows the NH_3-TPD results for the fresh and potassium-exposed H-BEA samples in the presence and absence of water. Fig. 1a shows the results in the presence of water, where a complete ammonia uptake can be observed for a few minutes followed by a sharp increase in the NH_3 response up to saturation with a small variation in the response for the different samples, thus difference in the total ammonia uptake. Furthermore, there is no significant difference between the samples during desorption of weakly bound ammonia, which is the ammonia desorbed during the first 30 min at constant temperature after

Table 2
Binding energies for Fe $2p_{3/2}$ and K 2p XPS peak maxima in various studies.

Species	Binding energy (eV)	Reference
Fe(II)O		
	709	Thomas et al., 1998 [54]
	709.5	McIntyre et al., 1977 and Moulder et al., 1992 [55,56]
	710.2	Pratt et al., 1997 [57]
	710.5	Janas et al., 2009 [58]
Fe(III)OOH		
	711.9	Moulder et al., 1992 [55]
$Fe(III)_2O_3$		
	711.6	McIntyre et al., 1977 [56]
	711	Thomas et al., 1998 [54]
	712	Thomas et al., 1998 [54]
	712.3	Janas et al., 2009 [58]
	712.7	Pratt et al., 2009 [57]
	714	Thomas et al., 1998 [54]
KNO_3	290	Moulder et al., 1992 [55]

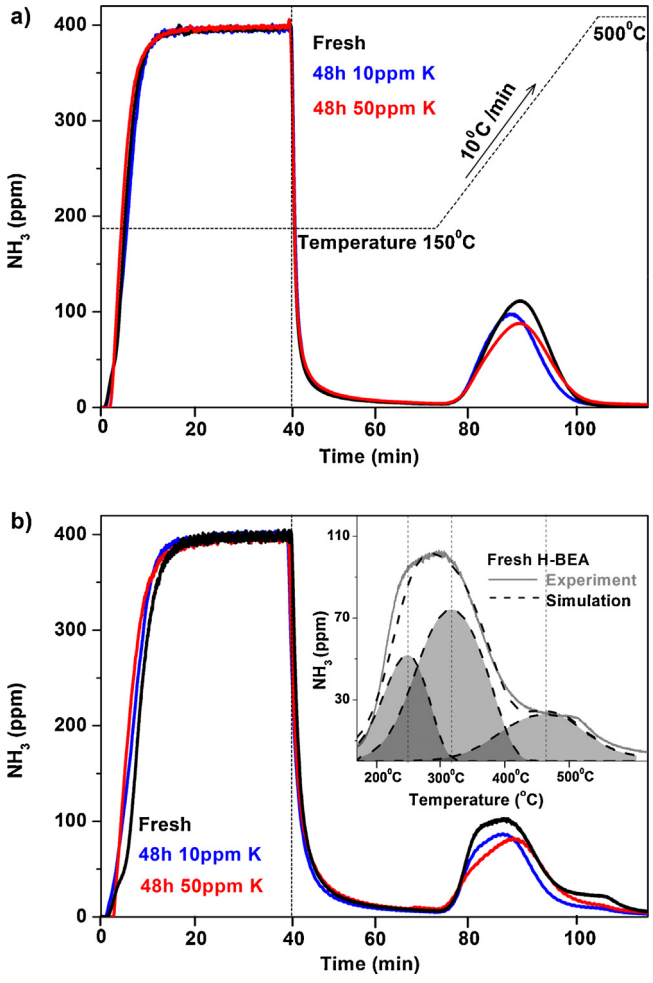

Fig. 1. NH_3 adsorption and desorption spectra for the studied H-BEA samples exposed to 10 and 50 ppm KNO_3 for 48 h: (a) in the presence of 5% H_2O and (b) in the absence of water. The samples were exposed to 400 ppm NH_3 for 40 min at 150 °C, flushed in Ar for 30 min and finally linearly heated to500 °C at 10 °C/min. The total flow rate was 3500 ml/min (GHSV = 27,600 h^{-1}). Simulation results from NH_3 desorption of different NH_3 adsorption sites of a fresh H-BEA sample is insetted in (b) from ref. [28]. Note that the temperature trace in (a) is valid also for (b).

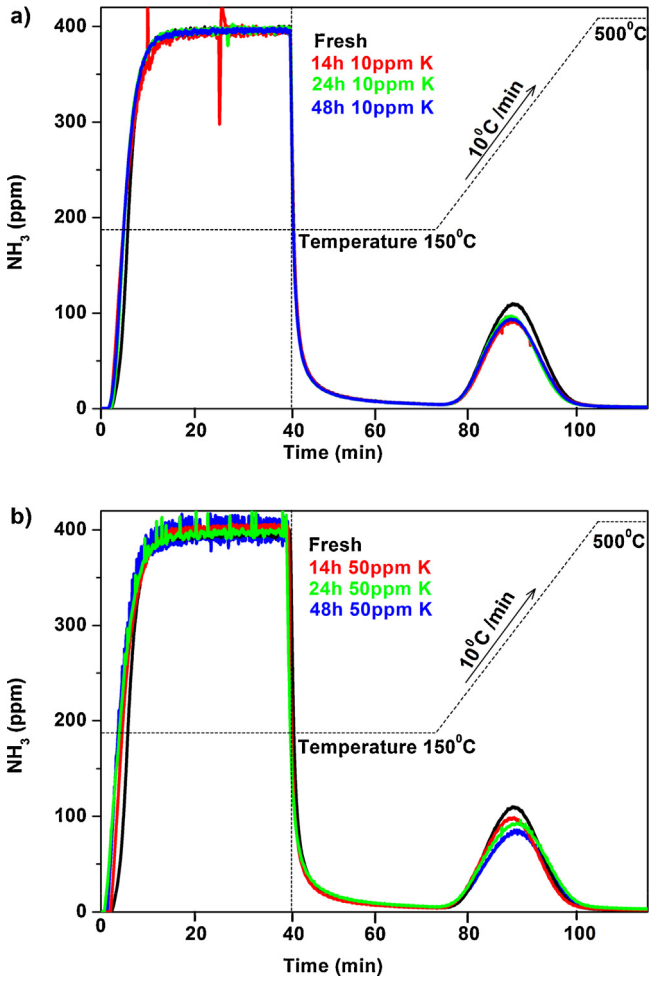

Fig. 2. NH_3 adsorption and desorption spectra for the studied Fe-BEA samples: (a) Catalysts exposed to 10 ppm KNO_3 for 14, 24 and 48 h. (b) Catalysts exposed to 50 ppm KNO_3 for 14, 24 and 48 h. The samples were exposed to 400 ppm NH_3 and 5% H_2O for 40 min at 150 °C, flushed in 5% H_2O in Ar for 30 min and finally linearly heated to 500 °C at 10 °C/min. The total flow rate was 3500 ml/min (GHSV = 27,600 h^{-1}).

the ammonia flow is cut off. However, there is a significant difference between the samples during the temperature ramp from 150 to 500 °C when strongly bound ammonia desorbs. The H-BEA sample exposed to 10 ppm potassium shows a significant decrease in the amount of NH_3 desorbed when compared to the fresh H-BEA sample. Furthermore, the desorption peak maximum shows a shift towards lower temperatures. The H-BEA samples exposed to 50 ppm potassium show a larger decrease in the total amount of desorbed ammonia. However, the desorption peak maximum shows a shift back towards higher temperatures, similar to the fresh H-BEA sample. Fig. 1b shows the results for the H-BEA samples in the absence of water. Furthermore, Fig. 1b shows the simulation results from a previously developed kinetic deactivation model [28,31] where the desorption peak for a fresh H-BEA sample is simulated using three different adsorption sites for ammonia in the zeolite. The simulation results show that the main desorption peak can be described by two Brønsted acid sites, one weak and one strong site, respectively [28]. The third site represents a Lewis site for relatively strongly bound ammonia which desorbs at higher temperatures [28,35]. Fig. 1b shows that the ammonia adsorption is significantly higher in the absence than in the presence of water. When the simulation results for the fresh H-BEA samples are compared to the desorption spectra of the potassium-exposed samples, there are some interesting notation. The results show that the decrease in magnitude of the desorption peak can be described by loss of both weak and strong Brønsted acid sites, and the loss of Lewis sites for the H-BEA sample exposed to 10 ppm potassium when compared to the fresh sample. However, the sample exposed to 50 ppm of potassium shows a different trend. The results indicate that weaker Brønsted sites are lost to a higher extent compared to the sample exposed to 10 ppm potassium.

Fig. 2 shows the results for the potassium-exposed Fe-BEA sample compared to a fresh Fe-BEA sample in the presence of water. Similar to the H-BEA samples, there is a complete uptake of ammonia for a few minutes followed by a sharp NH_3 response up to saturation. It can be observed in Fig. 2b that the samples exposed to 50 ppm potassium show a shorter complete ammonia uptake compared to the samples exposed to 10 ppm potassium. Furthermore, there is no clear difference between the amount of weakly bound ammonia for the Fe-BEA samples. However, during desorption of strongly bound ammonia, there is a significant difference between the samples. For the samples exposed to 10 ppm potassium in Fig. 2a, all samples show a decrease in ammonia storage capacity compared to the fresh sample. However, there is no significant difference between the potassium-exposed samples. Furthermore, for the samples exposed to 50 ppm potassium in Fig. 2b, the results show a difference between the potassium-exposed samples. The sample exposed to potassium for 14 h shows a decrease in storage capacity but no significant difference in desorption temperature of the peak maximum compared to the fresh sample. The samples exposed to potassium for 24 and 48 h show a more pronounced decrease in ammonia storage capacity and a shift in desorption maximum towards higher temperatures compared to the fresh and the less potassium-exposed sample.

3.2. Temperature-programmed desorption of NO

The results from the temperature-programmed desorption experiments using NO are shown in Fig. 3. Due to the low storage capacity of NO compared to NH_3, there is no complete uptake phase during the adsorption period nor any loosely bound NO desorbing after the NO cut-off, and therefore Fig. 3 only shows the desorption spectra of strongly bound NO. The fresh H-BEA sample does not show any desorption peak of NO, while the potassium-exposed H-BEA samples show an NO desorption peak. Furthermore, all Fe-BEA samples exposed to 10 ppm potassium show an increase in the NO storage capacity compared to the fresh Fe-BEA sample. For the Fe-BEA samples exposed to 50 ppm NO, there is a significant increase in the NO storage capacity for the sample exposed to potassium for 14 h, while the samples exposed for 24 and 48 h show a decrease in the NO storage capacity compared to the sample exposed for 14 h.

3.3. Temperature-programmed desorption of NO_2

Fig. 4 shows the desorption results from the temperature-programmed desorption of NO_2. Due to similar reason as for the NO-TPD experiments, only the NO_2 desorption spectra are shown in Fig. 4. The results show two distinct desorption peaks around 250 and 340 °C and a desorption shoulder around 430 °C. The fresh H-BEA and Fe-BEA samples do not show any significant peak around 250 °C compared to the potassium-exposed samples. Nevertheless, the potassium-exposed H-BEA samples show a significant increase in NO_2 desorption compared to the fresh sample for the peak around 250 °C. Furthermore, the Fe-BEA sample shows a clear increase in NO_2 desorption around 250 °C compared to the fresh Fe-BEA sample. However, the desorption peak around 340 °C decreases for both potassium-exposed H-BEA samples and the Fe-BEA samples exposed for 50 ppm of potassium. Furthermore, the desorption peak around 250 °C decreases for the samples exposed to 50 ppm of potassium for 24 and 48 h compared to the less exposed sample.

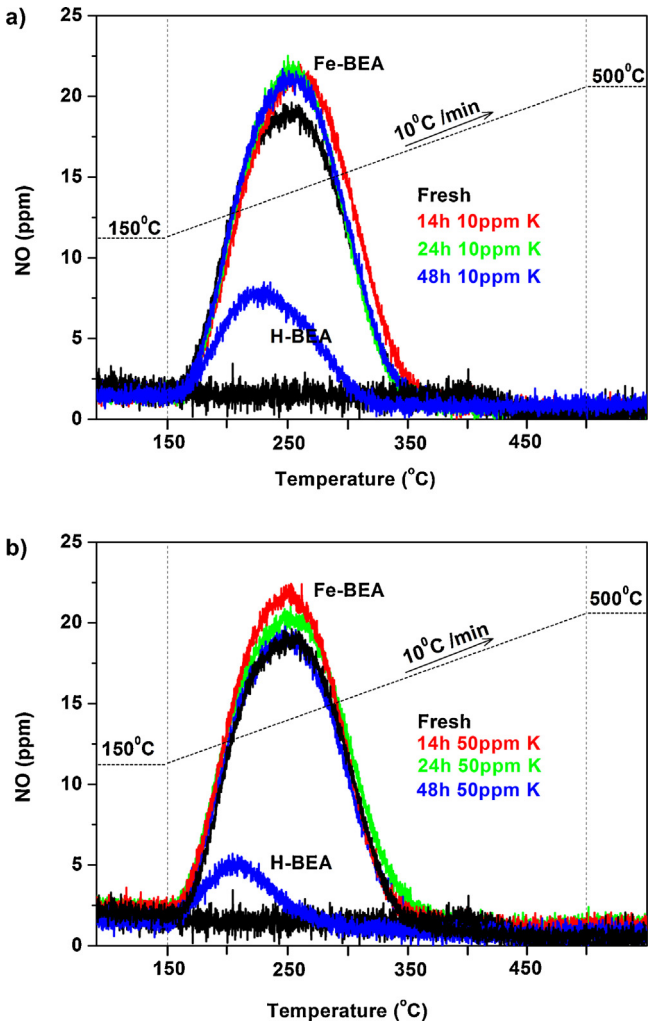

Fig. 3. NO desorption spectra for the studied H-BEA and Fe-BEA samples: (a) Catalysts exposed to 10 ppm KNO_3 for 14, 24 and 48 h. (b) Catalysts exposed to 50 ppm KNO_3 for 14, 24 and 48 h. The samples were exposed to 400 ppm NO for 40 min at 150 °C, flushed in Ar for 30 min and finally linearly heated to 500 °C at 10 °C/min. The total flow rate was 3500 ml/min (GHSV = 27,600 h^{-1}).

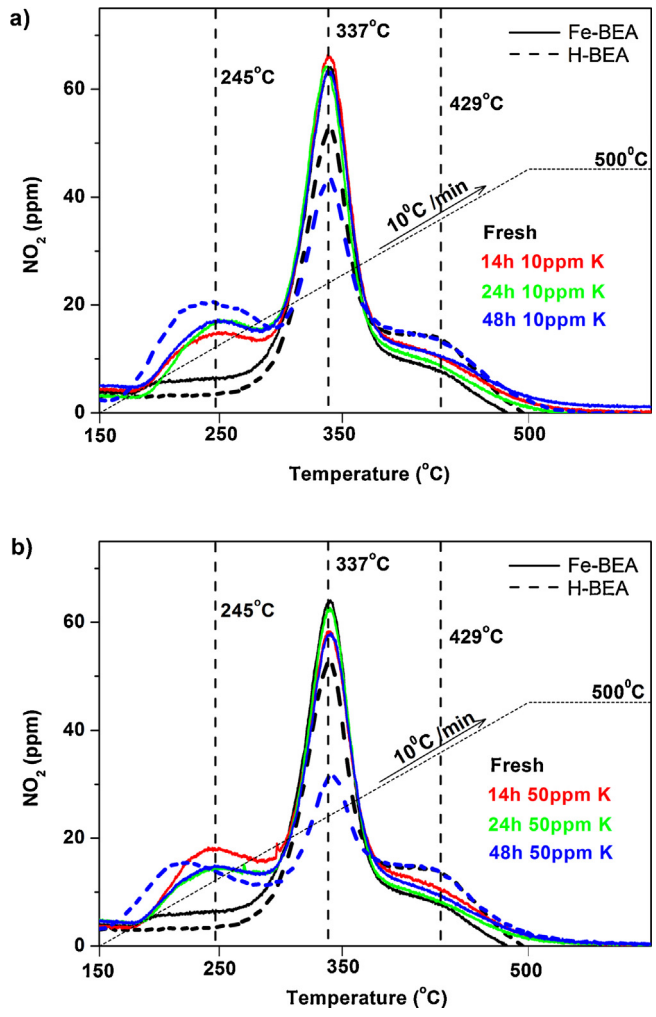

Fig. 4. NO_2 desorption spectra for the studied H-BEA and Fe-BEA samples: (a) Catalysts exposed to 10 ppm KNO_3 for 14, 24 and 48 h. (b) Catalysts exposed to 50 ppm KNO_3 for 14, 24 and 48 h. The samples were exposed to 400 ppm NO_2 for 40 min at 150 °C, flushed in Ar for 30 min and finally linearly heated to 500 °C at 10 °C/min. The total flow rate was 3500 ml/min (GHSV = 27,600 h^{-1}).

Furthermore, it should be mentioned that relatively small amounts of NO was observed during the adsorption period of NO_2. This is in agreement with previous studies of NO_2 storage where NO formation initially is observed during the adsorption period [36].

3.4. X-ray photoelectron spectroscopy

The XPS spectra for the fresh and potassium-exposed Fe-BEA samples are shown in Fig. 5 and the deconvoluted peaks from the experimental data are shown in Fig. 6. The K 2p peak overlaps with the strong and broad C 1s peak and therefore the results for the K 2p peak could not be evaluated and only the results for the Fe 2p peak are shown. Table 2 shows and summarizes the position of the Fe $2p_{3/2}$ peak for FeO, FeOOH and Fe_2O_3 from several studies.

Fig. 5 shows the XPS spectra of the Fe $2p_{3/2}$ peak with the positions marked for the deconvoluted Fe^{2+} and Fe^{3+} peaks. There is no clear shift in the peak position of the main Fe $2p_{3/2}$ peak when directly compared to the potassium-exposed samples. However, when comparing the deconvoluted spectra of the potassium-exposed and fresh Fe-BEA sample in Fig. 6 there is a clear difference between them. The area of the fitted peaks, attributed to Fe^{2+} and Fe^{3+} is marked with light and dark orange, respectively, in Fig. 6 and the ratio between them is for all Fe-BEA samples summarized in Table 1. For the fresh sample, the relative amount of Fe^{3+} is around 38%. The data in Table 1 show that the relative amount of Fe^{3+} increases for the potassium-exposed samples. For the samples exposed to 10 ppm potassium for 48 h, the relative amount of Fe^{3+} is around 44% compared to the fresh sample. However, the sample exposed to 50 ppm potassium for 48 h shows a more pronounced change in oxidation state compared to the samples exposed to 10 ppm potassium. For the Fe-BEA sample exposed to 50 ppm potassium for 48 h, the relative amount of Fe^{3+} is around 55%.

3.5. Oxidation of NH_3 and NO

The results from the NH_3 oxidation experiments at 500 °C are shown in Table 1. There is no significant ammonia oxidation activity at temperatures lower than 500 °C, hence only the results at 500 °C are shown in Table 1. The results show that there is no significant difference between the fresh and potassium-exposed H-BEA samples. However, the ammonia oxidation over the potassium-exposed Fe-BEA samples differs significantly compared to the fresh Fe-BEA sample. The Fe-BEA samples exposed shortest time for potassium, 10 and 50 ppm for 14 h, and show an increased activity for NH_3 oxidation compared to the fresh sample. Nevertheless, the samples

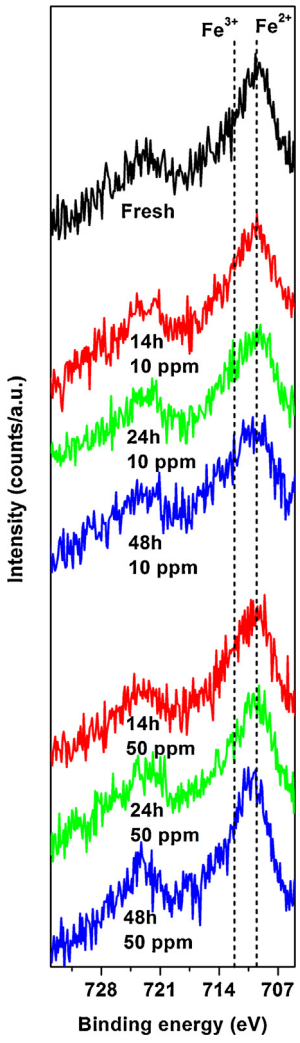

Fig. 5. XPS spectra of the Fe $2p_{3/2}$ and Fe $2p_{1/2}$ peaks of the potassium-exposed Fe-BEA samples compared to a fresh sample. The position of Fe^{2+} and Fe^{3+} is marked with dotted lines at 709.5 and 712.3 eV, respectively.

exposed to potassium for 24 and 48 h show a significant decrease in activity, where the sample exposed to 50 ppm potassium for 48 h shows an NH_3 conversion of 14% compared to 43% for the fresh sample.

The results from the NO oxidation experiments are not shown. There is no significant difference between the potassium-exposed samples neither when compared to the fresh samples. The Fe-BEA samples show the highest activity at 400 °C with an NO to NO_2 conversion of 16% and the H-BEA samples show the highest activity at 500 °C with 4% conversion of NO.

3.6. Selective catalytic reduction of NO_X with ammonia

The results from the selective catalytic reduction of NO_X using ammonia as a reducing agent are shown in Fig. 7. The figure shows the NO_X reduction after the reaction has reached steady state and no transient changes are observed at respective temperature. The potassium-exposed H-BEA samples show an increase in activity, especially at higher temperatures (>250 °C) when compared to the fresh H-BEA sample. However, the potassium-exposed Fe-BEA samples show a decreased activity compared to the fresh Fe-BEA sample over the entire temperature range. For the Fe-BEA samples exposed to 10 ppm of potassium, the least exposed sample (14 h) shows the highest decrease in activity. The Fe-BEA sample exposed for potassium for 24 and 48 h shows less decrease in activity compared to the sample exposed for 14 h. Furthermore, the Fe-BEA samples exposed to 50 ppm potassium show a stepwise decrease in activity from 14 to 48 h when compared. The sample exposed to 50 ppm for 14 h shows higher decrease in activity at higher temperatures (>200 °C) compared to the lower temperature range. However, the samples exposed for 24 and 48 h show a decrease in activity over the entire temperature range.

In general, all the potassium-exposed Fe-BEA samples show a decrease in activity over the entire temperature range, especially at temperatures higher than 200 °C. However, the H-BEA samples show the opposite trend. Both potassium-exposed H-BEA samples show an increase in activity, especially at temperatures higher than 250 °C.

3.7. Ammonia inhibition

The results from the ammonia inhibition experiments performed at 250 and 300 °C are shown in Fig. 8 and summarized in Table 1. The inhibition effect of ammonia is clearly seen for all samples at both temperatures. After the ammonia cut-off during the NH_3-SCR reaction, there is a period with immediate increase in NO_X reduction. For the H-BEA samples at 250 °C, the increased NO reduction period (until it passes the same level as prior to the NH_3-cut off) decreases compared to the fresh sample from 16 to 13 and 14 min for the samples exposed to 10 and 50 ppm potassium, respectively. For the potassium-exposed Fe-BEA samples, the trend with increased NO reduction period is similar. At 250 °C, the period with increased NO reduction decreases from 2.8 min for the fresh sample to 2.5 min for the sample exposed to 10 ppm potassium for 48 h.

At 300 °C, the increase in NO reduction period is significantly lower compared to at 250 °C. For the H-BEA samples, the increased NO reduction period decreases from 5.9 to 4.5 and 5.1 min for the samples exposed to 10 and 50 ppm of potassium, respectively. The Fe-BEA sample shows a decrease in NO reduction period from 0.9 to 0.5 min for the sample exposed to 10 ppm potassium for 48 h. However, the samples exposed to 50 ppm potassium show a lower decrease in NO reduction period compared to the samples exposed to 10 ppm potassium. The sample exposed to 50 ppm potassium for 48 h shows an increased NO reduction period for 0.7 min.

In general, the samples exposed to 50 ppm potassium show a lower decrease in increased NO reduction period after longer time of exposure compared to the samples exposed to 10 ppm potassium.

4. Discussion

4.1. NH_3 storage

The ammonia TPD experiments show a clear trend of decreased NH_3 storage capacity after potassium exposure. The storage capacity of ammonia in zeolites is mainly related to the Brønsted acidity of the zeolite and likely also to the number of iron sites in iron-exchanged zeolites [7,37–40]. This relationship is clearly seen when comparing the decreased storage capacity of ammonia and the dealumination of metal-exchanged zeolites due to hydrothermal treatment [30,31,39,41]. Kern et al. [15] showed a significant decrease in the ammonia storage capacity for an iron-exchanged zeolite impregnated with potassium nitrate solution. It was suggested that the decreased ammonia storage capacity was due to the plugging of the micro-pores of the zeolite. Our present results do not show any strong decrease in the ammonia storage capacity as shown by Kern et al. [15]. Nevertheless,

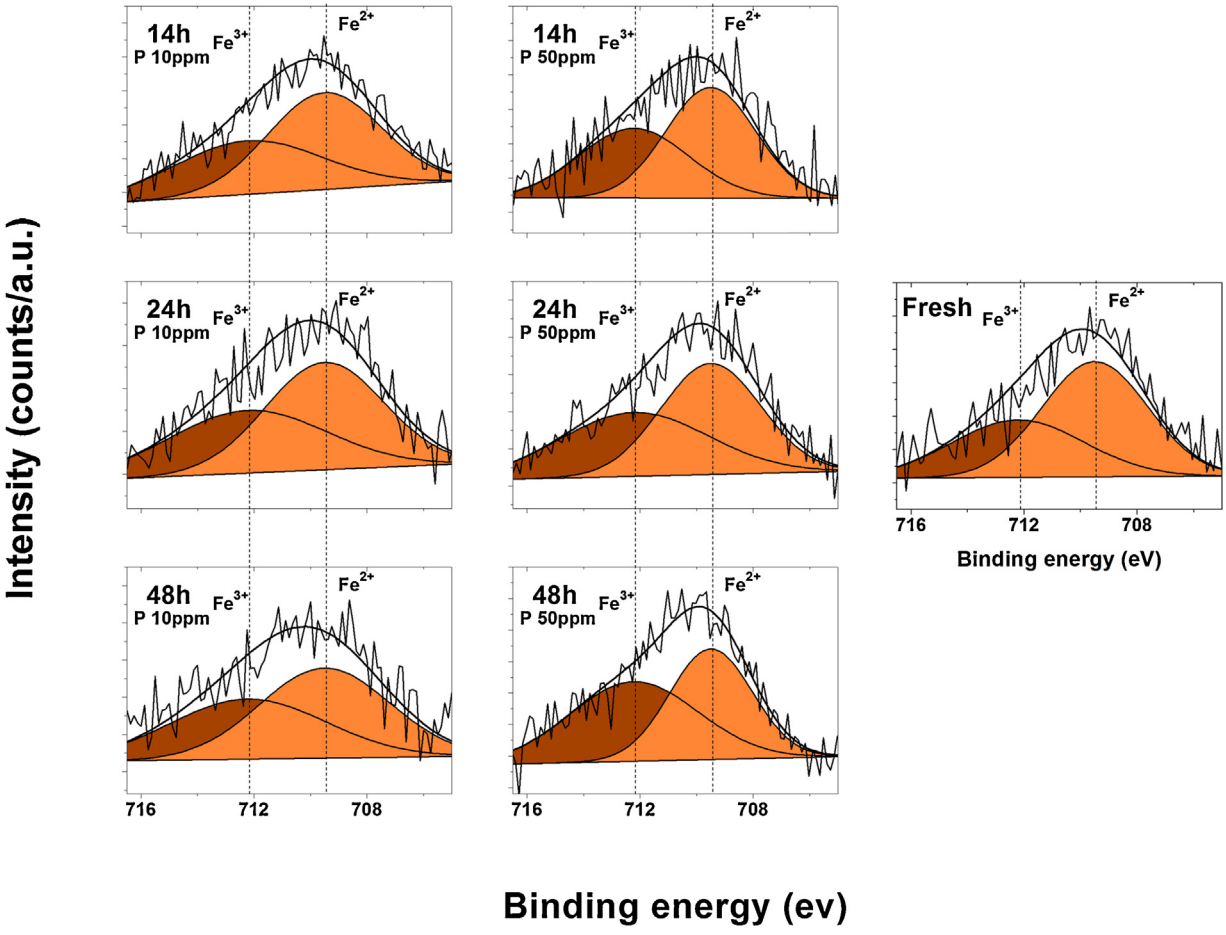

Fig. 6. Deconvolution of the Fe $2p_{3/2}$ XPS spectra of all potassium-exposed Fe-BEA catalysts compared to a fresh sample. The dark and light orange peak represents Fe^{3+} and Fe^{2+}, respectively. The sum of the deconvoluted peaks is shown by the solid black line and compared to the experimental data shown.

the NH_3 desorption maximum shows a shift towards lower temperatures for the samples exposed to less potassium compared to the samples exposed to higher amounts of potassium where the desorption peak was shifted towards higher temperatures. This could be explained by the NH_3-TPD experiments for the H-BEA samples performed in the absence of water, shown in Fig. 1b. The results show that after exposure to low amounts of potassium, both Brønsted sites decrease while exposure to higher amounts of potassium results in a more severe decrease of the weaker Brønsted sites compared to the stronger sites, resulting in a shift of the desorption maximum towards higher temperatures. The trend is similar for the iron-exchanged samples, where the ammonia desorption from the samples exposed to 50 ppm potassium shifts towards higher temperatures after longer time of potassium exposure. This indicates that potassium directly affects the two types of the Brønsted acid sites in the zeolite, where the weaker site is more severely affected, by hindering ammonia adsorption.

4.2. NO_X storage

The results in Figs. 3 and 4 show a clear trend in increased NO_X storage capacity of the potassium-exposed samples compared to the fresh samples. The fresh H-BEA sample does not show any NO storage capacity at all. However, after exposure to potassium, there is a significant storage capacity of NO in the zeolite. Similar results are observed for the potassium-exposed Fe-BEA samples, where an increase in the NO storage capacity is seen when compared to the fresh Fe-BEA sample, since no NO storage capacity was seen for the fresh H-BEA. However, the fresh Fe-BEA catalyst shows NO storage capacity due to iron sites [27,32]. This indicates that the increased storage capacity after potassium exposure is due to NO stored on new sites on the zeolite after potassium exposure. Furthermore, the NO_2 storage capacity increases significantly after exposure to potassium. The fresh H-BEA sample shows two distinct NO_2 desorption peaks which both are affected by the exposure to potassium. The desorption peak at higher temperature decreases as the desorption peak at lower temperature increases significantly at the same time. This indicates that potassium forms a new NO_2 storage site (at lower temperature) at the cost of the other NO_2 storage site (at higher temperature). The same trend is observed for the Fe-BEA samples where a new storage site for NO_2 is formed due to potassium exposure. Potassium is a well-studied NO_X storage component for NO_X storage catalysts [42–47]. Kobayashi et al. [46] studied the NO_X storage capacity of alkaline metals and found that potassium has the highest storage capacity. This could explain the increase in the storage capacity for the potassium-exposed H-BEA and Fe-BEA samples. Furthermore, the increase in the NO_X storage capacity appears to affect the number of Brønsted sites when correlated with the NH_3-TPD experiments. The NO_X storage sites seem to be formed on the expense of the Brønsted acid sites. Additionally, it can be observed that the samples exposed to 50 ppm potassium show slightly lower the NO_X storage capacity compared to the samples exposed to 10 ppm potassium, especially when studying the H-BEA samples. This indicates that some of the NO_X storage sites formed due to potassium exposure to some extent are temporarily and partially lost after exposure to higher amounts of potassium and longer exposure time.

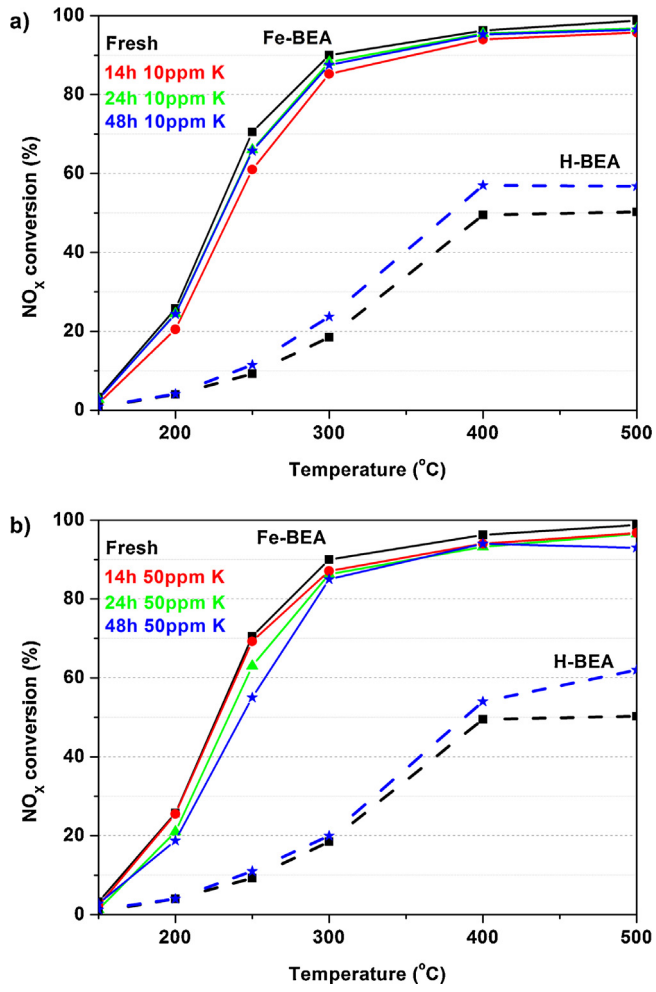

Fig. 7. Steady-state NO_X conversion of fresh and potassium-exposed H-BEA and Fe-BEA samples. (a) Catalysts exposed to 10 ppm KNO_3 for 14, 24 and 48 h. (b) Catalysts exposed to 50 ppm KNO_3 for 14, 24 and 48 h. The samples were exposed to 400 ppm NO, 400 ppm NH_3, 8% O_2 and 5% H_2O and the temperature was stepwise increased from 150 to 500 °C (150, 200, 250, 300, 400 and 500 °C). The total flow rate was 3500 ml/min (GHSV = 27,600 h^{-1}).

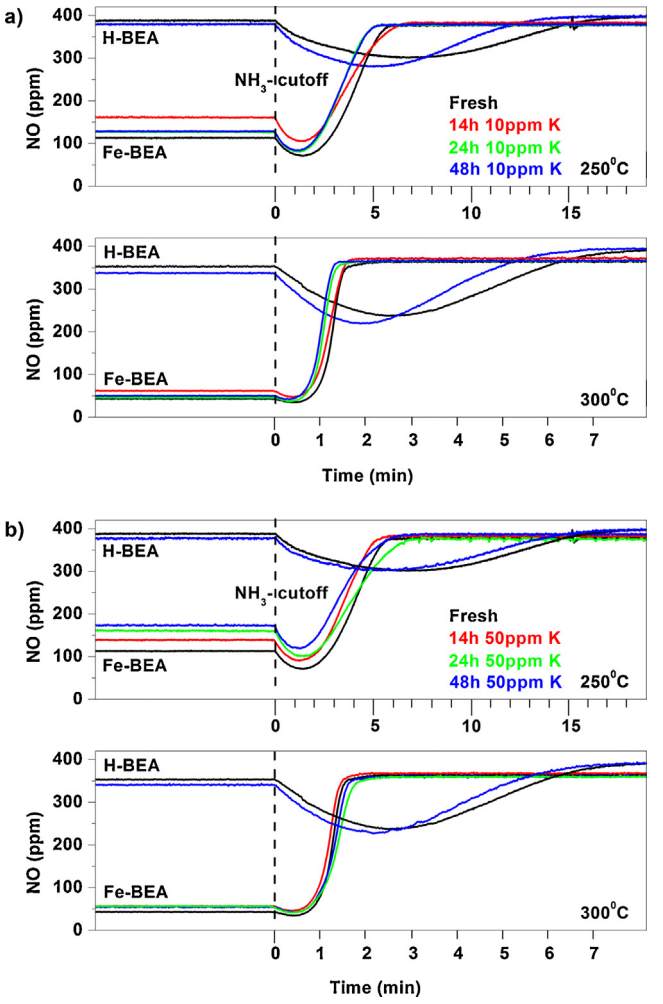

Fig. 8. Ammonia inhibition experiments for fresh and potassium-exposed H-BEA and Fe-BEA samples. (a) Catalysts exposed to 10 ppm KNO_3 for 14, 24 and 48 h. (b) Catalysts exposed to 50 ppm KNO_3 for 14, 24 and 48 h. The samples were exposed to 400 ppm NO, 400 ppm NH_3, 8% O_2 and 5% H_2O at 250 and 300 °C for 40 min. After 40 min, the gas mixture was kept unchanged except the NH_3 gas feed which was cut off. The NH_3-SCR activity was continuously measured before and after the ammonia cut-off. The total flow rate was 3500 ml/min (GHSV = 27,600 h^{-1}) and Ar was used as balance.

4.3. XPS

Table 1 summarizes the XPS measurements which clearly show a change in oxidation state of iron for the potassium-exposed Fe-BEA samples. The deconvolution of the Fe $2p_{3/2}$ peak shows that trivalent iron (Fe^{3+}) increases with potassium exposure, which represents monomeric iron (Fe^{3+}), iron particles (Fe_2O_3) and trivalent iron clusters (Fe_XO_Y) [19,27,30,32]. Previous UV–Vis measurements on the same catalyst [19] showed that monomeric iron is the dominating iron species in the catalyst, hence for the fresh Fe-BEA samples the Fe^{3+} peak represents primarily monomeric iron species. Nevertheless, after potassium exposure, the magnitude of the Fe^{3+} peak increases. A similar trend has previously been observed by our group after hydrothermal treatment of Fe-BEA [30,31]. It was concluded that the increase in Fe^{3+} results from formation of larger iron particles (Fe_2O_3) due to iron migration after hydrothermal treatment resulting in decreased NH_3-SCR activity. The migration of smaller iron species forming larger iron particles was further correlated to increased activity for NO oxidation which previously has shown to be the governing iron species for the oxidation of NO to NO_2 [48]. However, the NO oxidation experiments in the present study do not show any increase or change in NO oxidation activity after potassium exposure, hence the increase in the Fe^{3+} peak cannot be correlated to the formation of larger iron particles. The results show a decrease in activity over the entire temperature range, where monomeric iron species, Fe–O–OH (Fe^{3+}), are the governing iron species for low-temperature SCR and dimeric iron species, OH-Fe–O–Fe–OH (Fe^{2+}), the governing iron species for high-temperature SCR activity [49]. The decreased NH_3-SCR activity points towards loss of iron species active for NH_3-SCR. When correlating the XPS results with the activity measurements, it seems that exposure to potassium results in loss of monomeric and dimeric iron species and most likely formation of trivalent iron clusters (Fe_XO_Y) which have shown to not have any significant activity for NH_3-SCR [49]. This indicates that upon exposure to potassium, isolated iron species are exchanged with potassium, forming smaller iron clusters inside the zeolite pores. It is not likely that iron clusters migrate and form larger iron clusters or particles outside the zeolite pore due to the relatively low temperature (350 °C) when exposing the samples to potassium. Migration of iron inside zeolites has shown to occur at temperatures above 550 °C [7,30,39].

4.4. NH_3 and NO oxidation

The NH_3 oxidation experiments show a temporary increase in activity for the Fe-BEA samples with the shortest exposure time to potassium. Dimeric iron species, OH–Fe–O–Fe–OH (Fe^{2+}), have been shown to be the governing species for the oxidation of NH_3 [49]. The XPS results in the present study show a decrease in the relative amount of Fe^{2+} for the potassium-exposed samples which seems contradictory for the samples exposed to potassium the shortest time. However, the results in the present study indicate strong formation of new potassium sites which may temporarily affect the NH_3 oxidation activity. Nevertheless, after longer time of exposure to potassium, the NH_3 oxidation activity considerably decreases which can be correlated to the significant decrease in the relative amount of Fe^{2+} from the XPS results. As previously mentioned, larger iron particles (Fe_2O_3) have shown to be the governing species for the oxidation of NO to NO_2. In a recent study by our group, exposing Fe-BEA to phosphorous resulted in a stepwise decrease in activity during NO oxidation, indicating blocking of the iron particles [19] by phosphorous. However, the results from the present study do not show any changes in NO oxidation activity, indicating that the iron particles are not affected by the exposure to potassium and consequently not chemically blocked by potassium.

4.5. NH_3-SCR

The NH_3-SCR experiments show a clear deactivation for the Fe-BEA samples after exposure to potassium. However, the H-BEA samples show a significant increase in activity after potassium exposure. This can be correlated to the increased NO_X storage capacity of the zeolite. However, the increased activity for NH_3-SCR for the potassium-exposed zeolite (in H-BEA) does not seem to improve the SCR activity for the Fe-BEA samples. The potassium-exposed sample shows a significant decrease in SCR activity after 48 h of exposure. As mentioned in the previous section, this may be correlated to the XPS results which indicate loss of isolated iron species active for NH_3-SCR. The Fe-BEA sample exposed to 10 ppm potassium for 14 h shows the most severe deactivation of the samples exposed to 10 ppm potassium. The XPS results for this sample do not show the same magnitude in change of oxidation state which indicates that the new NO_X storage sites formed by potassium exposure might chemically block the iron sites active for NH_3-SCR after short time of potassium exposure while after longer time of exposure the active iron sites are physically lost and exchanged with potassium.

In general, the results indicate that for the potassium-exposed Fe-BEA sample, low amounts of potassium might chemically block the active isolated iron sites, while longer time of exposure results in exchange of the isolated iron species with potassium forming trivalent iron clusters, hence decreased NH_3-SCR activity. Furthermore, Ruggeri et al. [50,51] have discussed and showed that the oxidation of NO to NO_2 is not the rate limiting step in the standard SCR reaction for iron-exchanged zeolites. The results in the present work show a significant decrease in SCR activity after potassium exposure, but no changes in NO oxidation activity. These results are in line with mechanisms for standard SCR suggested by Ruggeri et al. [50,51]

4.6. Ammonia inhibition

High coverage of ammonia inhibiting the NH_3-SCR reaction is well known from previous studies of similar systems [7,10,37,52,53]. After ammonia is cut off, NH_3 spills over from the acid sites to the active SCR sites and reacts with adsorbed NO until all available stored ammonia is consumed. During this period, the NO conversion increases temporarily. The increased NO reduction period is strongly dependent on the total amount of ammonia stored in the catalyst. This might explain the difference in the increased NO reduction period between the samples exposed to 10 and 50 ppm potassium. The samples exposed to 50 ppm potassium during NH_3-TPD show a desorption peak maximum shifted towards higher temperatures which could explain the slightly longer increased NO reduction period compared to the samples exposed to 10 ppm potassium. The samples exposed to 50 ppm potassium release adsorbed ammonia slower than the samples exposed to 10 ppm potassium which increases the available ammonia for the SCR reaction after ammonia cut-off. Furthermore, the samples exposed to 50 ppm potassium have a lower steady-state activity for the SCR reaction, hence more ammonia is available during the transient step, which could further explain the longer NO reduction period. In a recent study of phosphorous exposure of Fe-BEA [19,33], the ammonia storage capacity increased while the increased NO reduction period significantly decreased indicating that the internal transport of ammonia was affected by chemical poisoning of phosphorous hindering adsorbed ammonia to participate in the SCR reaction. However, in the present study, the exposure to potassium does not seem to affect the internal transport of ammonia to the active SCR sites, but decrease the total amount of ammonia available due to chemical blockage or loss of Brønsted acid sites.

5. Concluding remarks

The objective of this study is to gain new fundamental understanding of the chemical deactivation mechanisms of H-BEA and Fe-BEA as NH_3-SCR catalysts after exposure to potassium. The focus is paid on the active iron sites and the interaction between potassium and the catalyst, and therefore the samples are exposed to relatively low amounts of potassium. The H-BEA and Fe-BEA samples are exposed to 10 and 50 ppm potassium nitrate between 14 and 48 h.

Temperature-programmed desorption experiments using ammonia, nitric oxide and nitrogen dioxide show that potassium exposure results in a significant increase in the NO_X storage capacity on the expense of Brønsted acid sites, which results in a decreased NH_3 storage capacity. The increased NO_X storage capacity results in increased NH_3-SCR activity for the potassium-exposed H-BEA samples. However, the potassium-exposed Fe-BEA samples show a significant decrease in NH_3-SCR activity. Deconvolution of the Fe $2p_{3/2}$ XPS peak for the Fe-BEA samples shows an increase in the relative amount of Fe^{3+} after exposure to potassium. The decrease in NH_3-SCR activity for the Fe-BEA samples is suggested to be due to loss of active isolated iron species after potassium exposure. The increase in the relative amount of Fe^{3+} indicates that isolated iron species form smaller trivalent iron clusters inside the zeolite pores. Furthermore, the ammonia inhibition experiments show a decreased period with improved NO reduction which is correlated to less available ammonia due to decreased storage capacity of NH_3.

In general, exposure to potassium results in increased NH_3-SCR activity for the H-BEA catalysts. However, potassium exposure results in chemical deactivation of Fe-BEA as NH_3-SCR catalyst due to exchange and loss of active isolated iron species with potassium in the zeolite. Furthermore, the deactivation is dependent on the availability of potassium used in the exposure treatment, which is more severe when using 50 ppm compared to 10 ppm potassium.

Acknowledgement

This work was performed within the FFI program (Project No. 32900-1), which was financially supported by the Swedish Energy

Agency and partly within the Competence Centre for Catalysis, which is hosted by Chalmers University of Technology and financially supported by the Swedish Energy Agency and the member companies AB Volvo, ECAPS AB, Haldor Topsøe A/S, Scania CV AB, Volvo Car Corporation AB and Wärtsilä Finland Oy. Financial support from Knut and Alice Wallenberg Foundation, Dnr KAW 2005.0055, is gratefully acknowledged. The authors would also like to thank Volvo Group Trucks Technology and Miroslawa Milh for help with the chemical deactivation of the samples.

References

[1] H. Sjövall, L. Olsson, E. Fridell, R.J. Blint, Appl. Catal. B: Environ. 64 (2006) 180–188.
[2] K. Rahkamaa-Tolonen, T. Maunula, M. Lomma, M. Huuhtanen, R.L. Keiski, Catal. Today 100 (2005) 217–222.
[3] S. Kieger, G. Delahay, B. Coq, B. Neveu, J. Catal. 183 (1999) 267–280.
[4] J.H. Park, H.J. Park, J.H. Baik, I.S. Nam, C.H. Shin, J.H. Lee, B.K. Cho, S.H. Oh, J. Catal. 240 (2006) 47–57.
[5] J.A. Sullivan, J. Cunningham, M.A. Morris, K. Keneavey, Appl. Catal. B Environ. 7 (1995) 137–151.
[6] H. Sjövall, E. Fridell, R. Blint, L. Olsson, Top. Catal. 42-43 (2007) 113–117.
[7] S. Brandenberger, O. Krocher, A. Tissler, R. Althoff, Catal. Rev. Sci. Eng. 50 (2008) 492–531.
[8] A. Grossale, I. Nova, E. Tronconi, D. Chatterjee, M. Weibel, J. Catal. 256 (2008) 312–322.
[9] A. Grossale, I. Nova, E. Tronconi, Catal. Today 136 (2008) 18–27.
[10] O. Kröcher, M. Devadas, M. Elsener, A. Wokaun, N. Söger, M. Pfeifer, Y. Demel, L. Mussmann, Appl. Catal. B: Environ. 66 (2006) 208–216.
[11] A. Grossale, I. Nova, E. Tronconi, Catal. Lett. 130 (2009) 525–531.
[12] K. Kamasamudram, N.W. Currier, T. Szailer, A. Yezerets, SAE Int. J. Fuels Lubr. 3 (2010) 664–672.
[13] C.H. Bartholomew, Appl. Catal. A: Gen. 212 (2001) 17–60.
[14] V. Kröger, Poisoning of Automotive Exhaust Gas Catalyst Components, Process and Environmental Engineering, University of Oulu, Oulu, Finland, 2007.
[15] P. Kern, M. Klimczak, T. Heinzelmann, M. Lucas, P. Claus, Appl. Catal. B: Environ. 95 (2010) 48–56.
[16] L. Ma, J.H. Li, Y.S. Cheng, C.K. Lambert, L.X. Fu, Environ. Sci. Technol. 46 (2012) 1747–1754.
[17] J. Li, R. Zhu, Y. Cheng, C.K. Lambert, R.T. Yang, Environ. Sci. Technol. 44 (2010) 1799–1805.
[18] C. He, Y. Wang, Y. Cheng, C.K. Lambert, R.T. Yang, Appl. Catal. A: Gen. 368 (2009) 121–126.
[19] S. Shwan, J. Jansson, L. Olsson, M. Skoglundh, Appl. Catal. B: Environ. 147 (2014) 111–123.
[20] R.G. Silver, M.O. Stefanick, B.I. Todd, Catal. Today 136 (2008) 28–33.
[21] T.R.C. Zezza, M.d.S. Castilho, N.R. Stradiotto, Fuel 95 (2012) 15–18.
[22] O. Kröcher, M. Elsener, Appl. Catal. B: Environ. 77 (2008) 215–227.
[23] F. Castellino, S.B. Rasmussen, A.D. Jensen, J.E. Johnsson, R. Fehrmann, Appl. Catal. B: Environ. 83 (2008) 110–122.
[24] D. Nicosia, I. Czekaj, O. Kröcher, Appl. Catal. B: Environ. 77 (2008) 228–236.
[25] F. Castellino, A.D. Jensen, J.E. Johnsson, R. Fehrmann, Appl. Catal. B: Environ. 86 (2009) 196–205.
[26] F. Castellino, A.D. Jensen, J.E. Johnsson, R. Fehrmann, Appl. Catal. B: Environ. 86 (2009) 206–215.
[27] S. Shwan, E. Adams, J. Jansson, M. Skoglundh, Catal. Lett. 143 (2013) 43–48.
[28] S. Shwan, R. Nedyalkova, J. Jansson, J. Korsgren, L. Olsson, M. Skoglundh, Top. Catal. 56 (2013) 80–88.
[29] R. Nedyalkova, S. Shwan, M. Skoglundh, L. Olsson, Appl. Catal. B: Environ. 138–139 (2013) 373–380.
[30] S. Shwan, R. Nedyalkova, J. Jansson, J. Korsgren, L. Olsson, M. Skoglundh, Ind. Eng. Chem. Res. 51 (2012) 12762–12772.
[31] S. Shwan, J. Jansson, J. Korsgren, L. Olsson, M. Skoglundh, Catal. Today 197 (2012) 24–37.
[32] S. Shwan, J. Jansson, L. Olsson, M. Skoglundh, Catal. Sci. Technol. 4 (2014) 2932–2937.
[33] S. Shwan, J. Jansson, L. Olsson, M. Skoglundh, AiCHE J (2014) 14638, http://dx.doi.org/10.1002/aic.14638.
[34] T. Yamashita, P. Hayes, Appl. Surf. Sci. 254 (2008) 2441–2449.
[35] C. Busco, A. Barbaglia, M. Broyer, V. Bolis, G.M. Foddanu, P. Ugliengo, Thermochim. Acta 418 (2004) 3–9.
[36] E. Fridell, H. Persson, B. Westerberg, L. Olsson, M. Skoglundh, Catal. Lett. 66 (2000) 71–74.
[37] S. Brandenberger, O. Kröcher, A. Wokaun, A. Tissler, R. Althoff, J. Catal. 268 (2009) 297–306.
[38] H. Sjövall, R.J. Blint, L. Olsson, J. Phys. Chem. C 113 (2009) 1393–1405.
[39] S. Brandenberger, O. Kröcher, M. Casapu, A. Tissler, R. Althoff, Appl. Catal. B: Environ. 101 (2011) 649–659.
[40] I. Nova, C. Ciardelli, E. Tronconi, D. Chatterjee, B. Bandl-Konrad, AiCHE J. 52 (2006) 3222–3233.
[41] S. Shwan, R. Nedyalkova, J. Jansson, J. Korsgren, L. Olsson, M. Skoglundh, Top. Catal. (2013) 1–9.
[42] Y. Tamura, S. Kikuchi, K. Okada, K. Koga, T. Dogahara, O. Nakayama, H. Ando, Development of Advanced Emission—Control Technologies for Gasoline Direct-Injection Engines, SAE International, USA, 2001, http://dx.doi.org/10.4271/2001-01-0254, Number: 2001-01-0254.
[43] D. Dou, J. Balland, Impact of Alkali Metals on the Performance and Mechanical Properties of NO_x Adsorber Catalysts, SAE International, USA, 2002, http://dx.doi.org/10.4271/2002-01-0734, Number: 2002-01-0734.
[44] T.J. Toops, D.B. Smith, W.P. Partridge, Appl. Catal. B: Environ. 58 (2005) 245–254.
[45] T.J. Toops, D.B. Smith, W.S. Epling, J.E. Parks, W.P. Partridge, Appl. Catal. B: Environ. 58 (2005) 255–264.
[46] T. Kobayashi, T. Yamada, K. Kayano, SAE Int. J. Engines 97-07-45 (1997).
[47] S. Salasc, M. Skoglundh, E. Fridell, Appl. Catal. B: Environ. 36 (2002) 145–160.
[48] M. Devadas, O. Kröcher, M. Elsener, A. Wokaun, G. Mitrikas, N. Söger, M. Pfeifer, Y. Demel, L. Mussmann, Catal. Today 119 (2007) 137–144.
[49] S. Brandenberger, O. Kröcher, A. Tissler, R. Althoff, Appl. Catal. B: Environ. 95 (2010) 348–357.
[50] M.P. Ruggeri, I. Nova, E. Tronconi, Top. Catal. 56 (2013) 109–113.
[51] M.P. Ruggeri, T. Selleri, M. Colombo, I. Nova, E. Tronconi, J. Catal. 311 (2014) 266–270.
[52] M. Wallin, C.J. Karlsson, M. Skoglundh, A. Palmqvist, J. Catal. 218 (2003) 354–364.
[53] A. Grossale, I. Nova, E. Tronconi, J. Catal. 265 (2009) 141–147.
[54] J.E. Thomas, C.F. Jones, W.M. Skinner, R.S.C. Smart, Geochim. Cosmochim. Acta 62 (1998) 1555–1565.
[55] J.F. Moulder, W. Stickle, P.E. Sobol, K.D. Bomben, Handbook of X-ray Photoelectron Spectroscopy, Perkin Elmer Corporation, Eden Prairie, MN, 1992.
[56] N.S. McIntyre, D.G. Zetaruk, Anal. Chem. 49 (1977) 1521–1529.
[57] A.R. Pratt, D.W. Blowes, C.J. Ptacek, Environ. Sci. Technol. 31 (1997) 2492–2498.
[58] J. Janas, J. Gurgul, R.P. Socha, T. Shishido, M. Che, S. Dzwigaj, Appl. Catal. B: Environ. 91 (2009) 113–122.